Variability of Cardiorespiratory Interactions Under Different Breathing Patterns

Dushko Lukarski[1,2], Dushko Stavrov[3] and Tomislav Stankovski[1,4*]

[1] *Faculty of Medicine, Ss. Cyril and Methodius University, Skopje, Macedonia*
[2] *University Clinic for Radiotherapy and Oncology, Skopje, Macedonia*
[3] *Faculty of Electrical Engineering and Information Technologies, Ss Cyril and Methodius University, Skopje 1000, Macedonia*
[4] *Department of Physics, Lancaster University, Lancaster LA1 4YB, United Kingdom*

Abstract

The breathing dynamics often change in time and cause different variations in the cardiorespiratory interaction. There exist various breathing patterns, among them one critically important is the variability of the breathing frequency. We investigated the respiratory and the coupled cardiorespiratory system under controlled time-varying breathing patterns. Four breathing scenarios were used for this: spontaneous breathing, one where the subjects changed their breathing frequency according to linear ramp law, another according to a sine law and third according to an aperiodic predefined law. We introduced a framework of variability measures to trace and quantify the effect from the time-varying breathing perturbations. In particular, we studied intra-subject time-average variability, inter-subject subject-average variability and residual variability. These variability measures were estimated from the coupling strength and the similarity of coupling functions, for which we used methods specifically able to follow the time-evolving dynamics – the time-frequency wavelet transform and the adaptive dynamical Bayesian inference. The results demonstrated that the coupling and similarity were significantly greater in controlled, compared to free spontaneous breathing in many cases ($p < 0.0083$). There were differences also among different controlled breathing regimes, and they appear both for intra-subject and inter-subject analysis. However, when the specific breathing perturbation is taken out, the results for the residual variability and the averaged coupling functions showed that the underlying interaction mechanisms remain invariant and not significantly different from spontaneous breathing ($p > 0.0083$). This variability framework carries implications and can be applied more generally to other coupled oscillators and networks.

Keywords: Cardiorespiratory interaction, Variability, Time-variability, Coupled oscillators, Coupling Function, Bayesian inference

*Corresponding author
t.stankovski@ukim.edu.mk

1. Introduction

The cardiovascular system has one of the central roles in the human body. Its functions are multifaced as it allows blood to circulate and transport nutrients to and from the cells in the body to provide nourishment and to help maintain homeostasis and fight diseases [1, 2]. The lungs and the heart, and how they interact, play very active role in mediating this mechanisms. As such, the cardiorespiratory interaction has been studied extensively in relation to different states and diseases [3, 4, 5, 6, 7, 8]. The cardiac and the respiration signals can be assessed by non-invasive measurements, making the investigations of cardiorespiratory interaction easily accessible. The dynamical activities of both the lungs and the heart have periodic oscillatory dynamics, which makes them very suitable for frequency and phase analysis and modeling.

As with many other biological thermodynamically-open systems, the cardiorespiratory system is also a subject to different *variabilities*. These result mostly from the non-isolated nature of the heart and the lungs, which exchange mater, electrical impulses and heat between themselves, other organs in the body and the environment. Arguably the most studied variability in the cardiovascular system is the Heart Rate Variability (HRV) and its association with the Respiratory Sinus Arrhythmia (RSA) [9, 10]. It describes the influence of the respiration frequency to the variability of the heart rate, and as such it represent one of the main and most important biomarkers in the analysis of the cardiovascular system [11, 12, 13, 14]. However, beside HRV, there are also other forms of variabilities which affect various aspects of the cardiovascular system, and in particular of the cardiorespiratory interaction.

In this paper we investigate different types of variabilities of the cardiorespiratory interactions as a result of predefined time-varying patterns of breading. In particular, we study the cardiorespiratory coupling functions variabilities and how they are affected during spontaneous free breathing and three time-varying patterns of breathing where the respiration frequency is changing according to: (i) linear ramp, (ii) sinus and (iii) aperiodic predefined law. The time-varying protocols were exactly identical for every subject. Because of this we were able to study inter-subject and intra-subject variabilities. Moreover, we also investigated time-varying residual variabilities i.e. if and how much the coupling functions vary when one excludes the average time-variability.

To investigate these variabilities under the time-varying protocols, we used a comprehensive framework of methods for analysis of oscillatory cardiorespiratory interactions. Importantly, the methods were able to follow the time-varying dynamics introduced as the specific perturbations to the cardiorespiratory system. First we used the time-frequency wavelet transform [15, 16, 17] to investigate the time-varying nature of the cardiac and respiration oscillations. Then we used a dynamical Bayesian inference method [5, 18] applied to the phase dynamics of the interacting cardiorespiratory oscillations. This method was able to infer the interacting phase dynamics, and with that to reconstruct the underlaying *coupling functions* [19, 20]. The cardiorespiratory coupling function describes in detail the mechanisms of how the respiration oscillation accelerates and decelerates the cardiac oscillation. We used a particular version of the dynamical Bayesian inference which is adaptive to the time-variability of the oscillations and can determine the optimal time window for the analysis [21]. The adaptive dynamical Bayesian inference was introduced only recently, and here we extend and deepen this approach to a detailed multi-subject analysis of the cardiorespiratory interactions under four different time-varying breathing patterns.

2. Material and methods

2.1. Subjects and breathing protocols

We investigated the cardiorespiratory interactions in 20 healthy subjects, with no known cardiorespiratory health issues. Of them, 13 subjects were male (age 26.2±7.5) and 7 were female(age 25.2±6.4). The investigation was approved by the Ethical Committee of the Medical Faculty at the University Ss. Cyril and Methodius in Skopje, Macedonia and a written consent was given by each of the subjects for participation in the study.

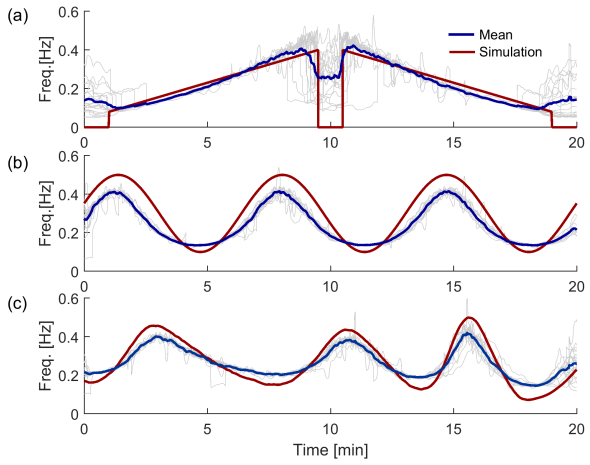

Figure 1: Comparison of the time-varying breathing frequency between the simulated reference and the mean frequency of all subjects. The thin grey lines represent the time-varying frequencies for the individual subjects. (a) presents the case for the ramp, (b) the sine and (c) the aperiodic controlled breathing. The instantaneous time-varying breathing frequency for each subject was extracted by wavelet ridge extraction [22].

The subjects respiration follows a predetermined breathing pattern by following a visual and audio computer simulation in which a ball is moved on a computer screen along a sine line. The frequency of the movement of the ball, together with the sine line, is varied according to the law we want the respiration to follow. At the maximum and the minimum of the sine line a beep is generated that marks the moments of maximal inhale and exhale of the subject. Fig. 1 shows how the subjects followed the specific time-variability during the controlled (a) ramped, (b) sine and (c) aperiodic breathing. There was small offset, particularly in (b) and (c) extremes, where the subjects did not followed very precisely the time-variability. This occurs possibly due to the adaptivity of the breathing process in respect to the presented sound and graphic breathing instructions. In the following variability analysis, only the introduced breathing time-variability is used i.e. the simulated reference is not part of the calculations. The measurements are performed by using the Biotec equipment with the subject lying in supine position. The respiration signal is obtained via an electric transducer on an elastic band placed on the chest of the subject, that measures the maximal and minimal circumference of the chest. The cardiac activity is followed by a three lead ECG measurement. The instantaneous cardiac phase is estimated from the ECG signal, while the respiratory phase from the respiratory signal.

The subjects respiration followed four breathing patterns: free breathing, breathing ramp, periodic breathing and aperiodic breathing. The duration of the free breathing was 30 minutes, while the duration of the other three breathing patterns was 20 minutes each, for each of the subjects. The breathing ramp consisted of one minute free breathing, followed by linearly increasing breathing frequency for 8.5 minutes from 0.08Hz to 0.4 Hz, then one minute of free breathing, than linearly decreasing breathing frequency for 8.5 minutes from 0.4 Hz to 0.08 Hz. The periodic breathing pattern followed a sine law change of the frequency, given by the equation $f = 0.3 + 0.2sin(2\pi t/400)$. The aperiodic breathing pattern followed the z-component of a chaotic Lorenc system [23].

2.2. Wavelet transform

After the measurement and the visual check of the signals for each of the subjects, we first analysed the time series by using the continuous wavelet transform [15, 16, 17]. For a given signal $x(t)$, the continuous wavelet transform is given with the equation

$$WT(\omega, t) = \int_0^\infty \psi(\omega(u-t))x(u)\omega du. \qquad (1)$$

where, ω denotes the angular frequency, t is the time, and

$$\psi(u) = \frac{1}{2\pi}(e^{j2\pi f_0 u} - e^{\frac{(2\pi f_0)^2}{2}})e^{-\frac{u^2}{2}}$$

is the complex Morlet wavelet, with central frequency $f_0 = 1$, $\int \psi(t)dt = 0$, and with i being the imaginary unit. It is a time-frequency representation containing both the phase and the amplitude dynamics of the oscillatory elements from the analyzed signal and it is used to check whether the subjects respiration followed the desired pattern.

2.3. Adaptive Dynamical Bayesian Inference

In the study of dynamic systems, knowledge of their temporal changes is usually acquired by analyzing the time series of measured signals emanating from them. Dynamical inference methods make it possible to describe such systems as a solution of a system of differential equations. Typically, the inference methods involve a hypothetical model that describes the phenomenon and consists of determining the parameters of the model that describe the system and the interactions within. The dynamical systems of interest for this research are the oscillatory systems of the human body.

According to the phase reduction theory, when the interaction between two oscillators is sufficiently week, their motion can be approximated by their phase dynamics [24, 25]. When the phases of the system can be regarded as monotonic change of the variables, the dynamical process can be represented with the system of differential equations:

$$\dot{\varphi}_i = \omega_i + q_{i,j}(\varphi_i, \varphi_j) + \xi_i, \tag{2}$$

where φ_i is the phase of the i-th oscillator, ω_i is its angular frequency parameter, $q_{i,j}$ is the coupling function describing the influence of the j-th oscillator on the i-th oscillator and ξ_i represents the noise. A common assumption for the noise is that it is white Gaussian noise given by $\xi_i(t)\xi_j(\tau) = \delta(t-\tau)E_{ij}$, where the symmetric matrix E_{ij} incorporates the information about the correlation between the noises of the different oscillators.

Because the system is periodic in nature, the coupling function can be represented by a Fourier decomposition:

$$q_{i,j}(\varphi_i, \varphi_j) = \sum_{k=1}^{\infty}\sum_{s=1}^{\infty} c_{i;k,s} e^{i2pk\varphi_i} e^{i2ps\varphi_j} \tag{3}$$

For a system of two coupled oscillators, reduction to a finite number K of Fourier terms gives:

$$\dot{\varphi}_i = \sum_{k=-K}^{K} {c_k}^i \Phi_{i,k}(\varphi_i, \varphi_j) + \xi_i(t), \tag{4}$$

where $i = \{1, 2\}, \Phi_{1,0} = \Phi_{2,0} = 1, {c_0}^i = \omega_i$ and the rest $\Phi_{i,k}$ and ${c_k}^i$ are the K most important Fourier components (in this work we used $K = 2$). With the assumption for a white Gaussian noise, the task is then reduced to inference of the unknown parameters of the model:

$$M = \left\{ {c_k}^i, E_{ij} \right\}, \tag{5}$$

from where the coupling functions $q_{i,j}$ are determined, and with that the underlaying interaction mechanisms [19].

In the method of adaptive dynamical Bayesian inference (aDBI), the time series of phases of the oscillators are considered to be time sequences of blocks of samples. Each block includes the samples from a certain time interval whose duration is specified by the time window t_w. For each block Bayesian inference is performed and the values for the parameters of the model and the couplings are obtained [5, 26, 27, 21]. The initial assumptions for the model parameters are that ${c_k}^i = 0$ and therefore at least few inference blocks are required to obtain appropriate estimates of the model parameters values and the corresponding coupling functions. The method provides the values of the parameters for each block of inference, which allows monitoring the time evolution of the system, with a temporal resolution defined by the time window t_w. The output values of the previous block are used as input values for the next block of inference and in each subsequent step, part of the information obtained from the previous step is included.

How much of this information is included in the current inference is determined by the so-called propagation parameter p_w, which is closely related to the duration of the time window t_w. In the method of aDBI both of these parameters are adaptively determined, based on the time variabilities present in the signal. As a first step, an initial inference is performed, with a small value for the time window and a fixed value for the propagation parameter $p_w = 0.2$. This initial value of the time window is selected to be as small as possible, in order to infer the time changes of the parameters with the highest possible time resolution, but at the same time not to be so small that method calculation does not break. By using such values for t_w and p_w, an initial estimation of the

model parameters is obtained, which describes the parameter dynamics with high temporal resolution, but with high noise as well. From the dynamics of these initial parameters and with the help of their fast Fourier transform, the highest frequency of change of the parameters f_{max} is determined. Then, the optimal time window is calculated by making the assumption that for accurate description of the fastest changing parameter at least 8 blocks per oscillation period T_{min} are needed, hence $t_{w,opt} = \frac{T_{min}}{8} = \frac{1}{8f_{max}}$. From the determined optimal time window, the optimal propagation parameter is obtained as:

$$p_{w,opt} = \begin{cases} 0.1, & t_{w,opt} > 40 \\ 0.2, & t_{w,opt} \in [10, 40] \\ \frac{2}{t_{w,opt}}, & t_{w,opt} < 10. \end{cases} \quad (6)$$

These values for the optimal propagation parameter are obtained from studies of coupled phase oscillators with frequencies in the cardiorespiratory range, by minimizing the covariance matrix [21]. After determining the optimal values for the time window and the propagation parameter, a second inference is performed. For this inference the covariance matrix is smaller, preserving at the same time the appropriate tracking of the time variability of the parameters and the coupling functions.

After the initial wavelet observation of the oscillations, a phase extraction procedure is performed to obtain the instantaneous phase time-series which act as input to the aDBI method. First the oscillatory intervals are evaluated by standard digital filtering procedure including FIR filter followed by a zero phase filtering procedure ("filtfilt") to ensure that no time or phase lags are introduced with the filtering procedure. The respiratory signal limits are from 0.08Hz to 0.8 Hz, while for the ECG signal are from 0.6 Hz to 2 Hz. The phases of the filtered signals are estimated via Hilbert transformation, thus obtaining the protophases. On these protophases, we apply the prtophase-to-phase transformation [28] in order to obtain the independent phases.

2.4. Coupling functions

Interactions between dynamical systems in nature are defined by two main aspects - their structure and their function. One way of describing the functional mechanisms is by using coupling functions [19]. Coupling functions describe the physical laws that govern the interactions of systems and therefore, knowledge of coupling functions can be used to register or predict a physical effect that originates in the interactions between systems.

The coupling function can be described by its strength and its form. The coupling strength describes the extent and the range of the coupling, while the form of the coupling function contains the law that describes the impact from one of the subsystems onto the other. In theoretical considerations, the coupling strength is the scaling parameter of the coupling functions. When the coupling function is comprised of several components, as is the case in periodic dynamics decomposed in Furies components, its net coupling strength is usually evaluated as an Euclid's norm of the strengths of the individual components: $\varepsilon(t) = \sqrt{c_i^2 + c_j^2 + ... + c_K^2}$. For quantitative statistics we also report the median of the coupling strength of the subject group, which we denote as $\bar{\varepsilon}$.

As for the quantification of the functional form, one of the ways is the use of correlation coefficients applied on the inferred coupling parameters [6]. The measure of similarity index, ρ, gives the similarity between two coupling functions q_1 and q_2, regardless of their coupling strengths. This index is determined as the correlation coefficient:

$$\rho = \frac{\langle \tilde{q}_1 \tilde{q}_2 \rangle}{\|\tilde{q}_1\| \|\tilde{q}_2\|}, \quad (7)$$

where $\langle q \rangle$ denotes spatial averaging over a two dimensional domain $0 \leq \varphi_1, \varphi_2 \leq 2\pi$, and $\tilde{q} = q - \langle q \rangle$ and $\|q\| = \langle qq \rangle^{1/2}$. For quantitative statistics the median of similarity index was denoted as $\bar{\rho}$.

2.5. Statistical analysis and surrogate data

When analysing oscillatory signals, the inferred coupling between the signals is always positive and non-zero, even if the oscillators are uncoupled or unrelated. Therefore, it is necessary to establish a significance threshold in order to determine if the obtained coupling indicates a genuine connection and

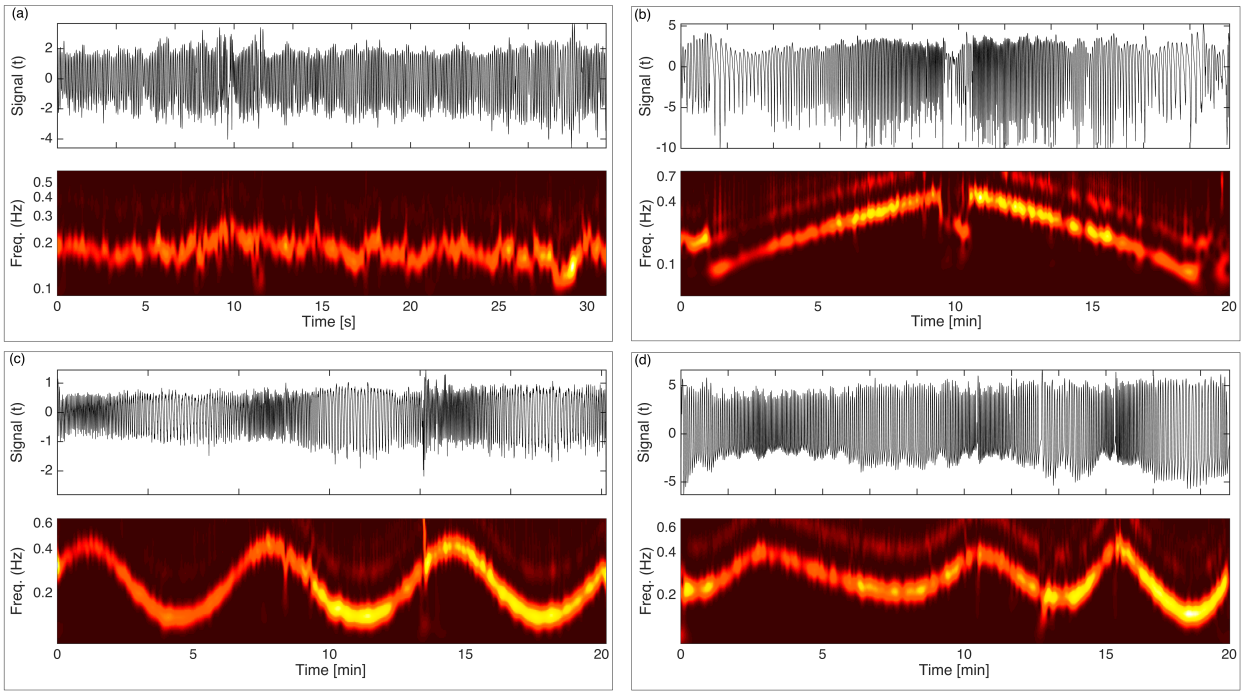

Figure 2: The time and time-frequency wavelet transform of the respiration oscillations during four breathing patters. The plots in (a) represent free spontaneous breathing, in (b) linear ramp breathing, in (c) sine breathing and in (d) aperiodic breathing of a single subject.

interdependence of the phenomena. Such a threshold is usually defined by constructing randomized surrogates of the original signals [29, 30] and calculating the coupling functions for these surrogates. The coupling functions obtained in this manner represent a baseline for the confirmation of the coupling of the oscillators. In this work we used surrogates constructed by rearranging the cycles within the extracted phase, a procedure referred to as cycle phase permutation surrogates [30]. The surrogate threshold is taken to be the mean plus two standard deviations (mean+2STD) of the surrogate couplings.

For statistical analysis and comparison of different distributions we used the standard nonparametric Wilcoxon statistical test. To present the differences between the distributions visually, we use standard boxplots which refer to the descriptive statistics (median, quartiles, maximum and minimum). Due to the multiple comparisons we used the Bonferroni correction. There were six unique hypothesis combinations, therefore the Bonferroni correction resulted in *alpha* value of $\alpha = 0.05/6 = 0.0083$, leading to the significance level of $p < 0.0083$.

3. Results

The results present a comprehensive analysis of the interacting oscillations. First we observe the existence, strength and the time-variability of respiration oscillations using the time-frequency wavelet transform. Then we analyse in more detail the cardiorespiratory coupling, observing the coupling strength, the coupling functions and their respective statistical differences due to different breathing patterns.

The nature of the respiration oscillations for the four breathing patterns are presented on Fig. 2. Each block on the figure represents the respiratory signals in time (top plot) and the corresponding time-

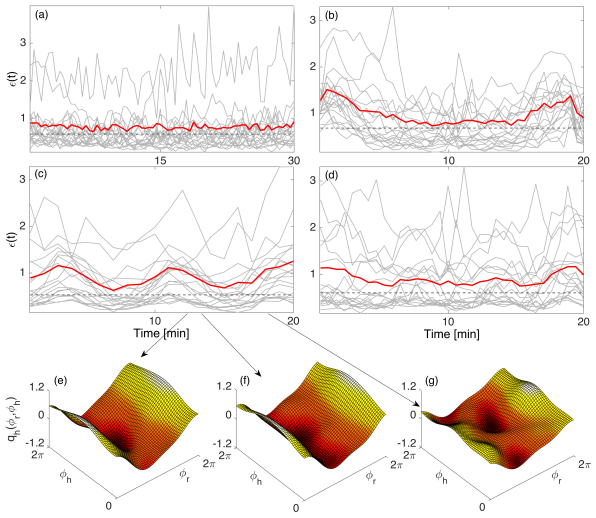

Figure 3: Cardiorespiratory coupling strength and its time-variability according to the four breathing patterns – spontaneous (a), ramp (b), sine (c) and aperiodic breathing (d), respectively. The grey thin lines present the coupling strengths of the individual subjects, while the thick over-line is the group mean. The dashed lines represent the surrogate threshold. The three plots (e), (f) and (g) show subject-averaged (inter-subject) coupling functions for three specific time instances from the sine breathing pattern, as indicated by the arrows.

frequency wavelet transforms (bottom plot). The four blocks on Fig. 2 represent the spontaneous breathing Fig. 2 (a), and the three breathing perturbations for the ramp breathing Fig. 2 (b), the sine breathing Fig. 2 (c) and the aperiodic breathing Fig. 2 (d). By observing and comparing the four wavelet plots, one can notice that the subject free spontaneous breathing spans narrow frequency interval and there are many spontaneous variabilities, while during the three controlled regimes with the ramp, sine and aperiodic patterns the frequency variations span in a regular manner over a wider frequency interval, as intended by the experimental protocol. In general, the subjects were able to follow the proposed breathing protocols quite precisely.

After observing the wavelet oscillations, we move to inference of the phase dynamics. The adaptive determination of the time window and the propagation parameter gave qualitatively different results for the spontaneous breathing and for the breathing following predetermined respiration pattern. Namely, when the breathing follows a predetermined pattern where certain frequencies dominate, as is the case with the periodic and aperiodic breathing pattern, than for all subjects the aDBI gives the same values for the optimal time window and propagation parameter. For the case of periodic breathing pattern, the optimal values are $t_{w,opt} = 52s$ and $p_{w,opt} = 0, 1$, while for the aperiodic breathing pattern $t_{w,opt} = 32s$ and $p_{w,opt} = 0, 2$. For the free breathing and for the ramp breathing pattern, which includes 3 minutes of free breathing, there is a certain variability between the subjects in the optimal parameter values. For the case of free breathing $t_{w,opt} = (24 \pm 8)s$ while for the case of ramp breathing pattern $t_{w,opt} = (27 \pm 7)s$. For both cases the propagation parameter has value $p_{w,opt} = 0, 2$. For the further analysis the mean values of the time windows are used.

The coupling from the respiration to the heart had distinct time-variability during the four characteristic breathing regimes – Fig. 3. Before going into qualitative evaluation, one needs first to compare and validate the coupling strength levels with the corresponding surrogate thresholds (horizontal dashed blacked lines in all the plots on Fig. 3). From all the four plots in Fig. 3 one can notice that the average coupling strength (thick lines) are close but always above the surrogate thresholds. This indicates that on average the detected cardiorespiratory coupling was statistically significant in respect to surrogates. However, it was interesting to find that the coupling for some subjects (thin grey lines) was often below the threshold for some time intervals. In some cases this intermittent surrogate-significance followed the specific time-varying breathing patterns. This showed that the cardiorespiratory coupling was not only increasing and decreasing, but often it was also changing from being to not being statistically significant, meaning it was like appearing and disappearing coupling.

Observing and comparing the specific time-variability on the different breathing patterns one can notice that during the free spontaneous breathing Fig. 3 (a) the average coupling strength was (almost) invariant without some large deviations and variabilities. The ramp breathing Fig. 3 (b) followed the

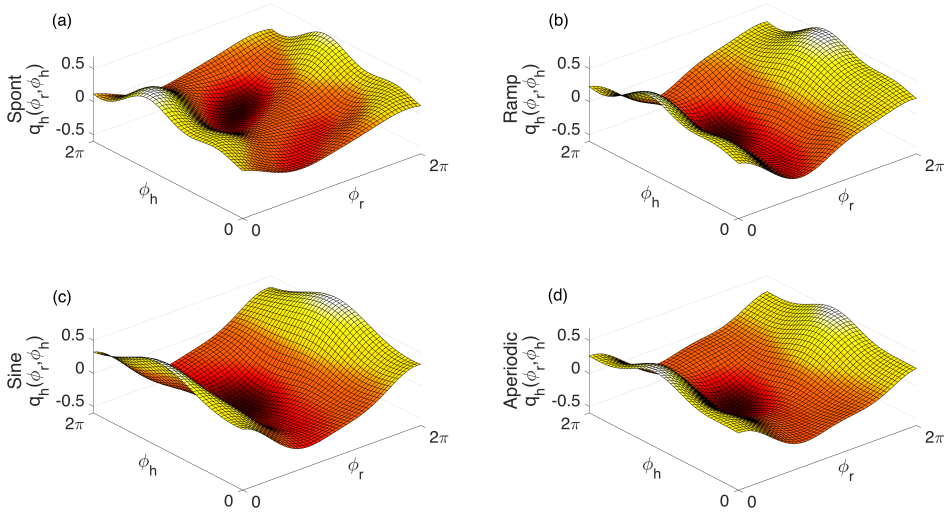

Figure 4: Cardiorespiratory coupling functions for the four different breathing regimes. Each plot shows the coupling function as group average among subjects. The coupling functions are calculated for the respiration to heart interaction modelled from their respective phase dynamics. As previously, the cardiorespiratory coupling functions are presented for the (a) spontaneous, (b) ramp, (c) sine and (d) aperiodic breathing pattern. Note that for comparison, all the coupling functions are presented on the same scale on the z-axis.

breathing protocol in a sense that the coupling was first decreasing and than increasing. The variabilities were close to, but not fully linear as the introduced ramp experimental variabilities of the frequencies. Arguably, the coupling strength was following best the time-variability of the periodic sine breathing in Fig. 3 (c). The aperiodic breathing introduced coupling strength (Fig. 3 (d)) which was similar, but not so close and very varying in comparison to the aperiodic breathing frequency. In general, the average coupling strength from all three breathing patterns followed inversely the introduced time-variabilities of the respiration frequency (compare Fig. 2 and Fig. 3) i.e. for low-frequency breathing there was high coupling, while for high-frequency breathing there was low coupling.

Next we analysed the cardiorespiratory coupling functions, or how the respiration affects the cardiac oscillations. In general, we observed time-variabilities of the form of the coupling functions as the breathing patterns changed, similarly as it has been shown before for cardiorespiratory [5, 21] and neural [31] coupling functions. These variabilities were both in time and among subjects. In Fig. 3 (e), (f) and (g) we show how the subject-averaged coupling functions evolve in time. By comparison, one can notice that the time-consecutive Fig. 3 (e) and (f) have much similar shapes, while Fig. 3 (g) evaluated later in time is much more variable and different in form than the other two in (f) and (g). Similar to these subject-variability, the time-variability were arguably even greater.

However, when we time-averaged and subject-averaged the coupling functions, we found a different pattern. Fig. 4 shows the time and subject average coupling functions for the different breathing patterns. If we compare all the coupling function in Fig. 4 (a)-(d), we can notice that they all have very similar form of the functions. The spontaneous coupling function in Fig. 4 (a) is slightly more variable in comparison to the other three during controlled breathing, but again in general all four of them are qualitatively very similar. This implies that, the individual and time-dependent differences that appear in the variabilities of the coupling function are all averaged-out. The specific form of the coupling function shown in Fig. 4 (a)-(d) reveals the interaction mechanism in detail i.e. that the coupling depends predominantly only on the direct influence from respiration, revealing how when the function increases or decreases along the respiration axis, the heart oscillations are accelerated or decelerated, respectively.

After we observed the qualitative characteristics on the coupling functions, we move to in-depth statis-

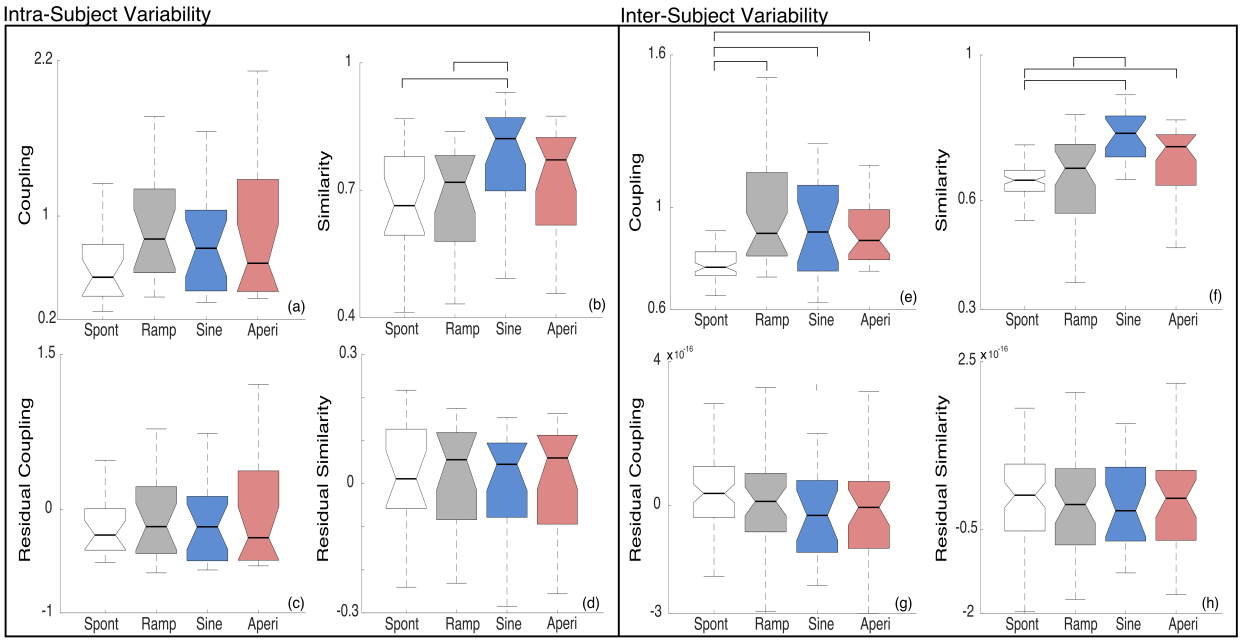

Figure 5: Statistical analysis of cardiorespiratory variabilities in relation to the different modes of breathing. Each plot (a)-to-(h) shows four color-coded boxplot distributions for the spontaneous, ramp, sine and aperiodic breathing, respectively. There are two groups of variabilities: intra-subject (a)-(d) and inter-subject (e)-(h) variability, each indicated with box grouping four specific plots. The variabilities are calculated as averages of the coupling (strength) and the similarity (of forms of coupling functions) measures. The plots in the top row (a),(b),(e) and (f) are calculated for the regular values, while in the bottom row (c),(d),(g) and (h) are the calculated residual variability. Importantly, the lines over the boxplots indicate existence of statistical difference ($p < 0.0083$) between two boxplot distributions.

tical analysis of the their quantitative characteristics. Here we studied two measures – the coupling strength and the index of similarity of coupling functions. The results for the different breathing patterns, along with evaluation of their statistical differences are shown in Fig. 5. We studied the results through two complementary variabilities: intra-subject and inter-subject. Namely, for the intra-subject analysis we *time-average* the signals within each subject (thus called 'intra'). For example, for one subject we have the inferred coupling strength time-series (like the grey lines in Fig. 3) and then we take the mean of the this time-evolving coupling to get a single value; then a boxplot shows the distribution of these values for all the subjects for some breathing pattern. The inter-subject analysis, on the other hand, refer to *subject-average* of the values for specific time for all subjects. We are able to do this because all the subjects during the controlled breathing followed exactly the same protocol. For example, at some time window, we average the coupling strength values from all the subjects at that time; then a boxplots shows a distribution of these values for all the time-windows for some breathing pattern. All the analysis on Fig. 5 is done for the average mean values, and we have done also analysis for the standard deviations of the same variables. The trends and conclusions were similar for the resulting figure with standard deviation analysis, which is shown in the Supplementary materials.

The intra-subject coupling in Fig. 5 (a) shows that all the controlled breathing patterns (ramp (median coupling strength $\bar{\varepsilon} = 0.8226$), sine ($\bar{\varepsilon} = 0.7512$) and aperiodic ($\bar{\varepsilon} = 0.6355$)) are greater than the sponta-

neous breathing on average ($\bar{\varepsilon} = 0.5276$), however, this was not statistically significant ($p > 0.0083$). Then, for the similarity index in Fig. 5 (b) the sine breathing ($\bar{\rho} = 0.8709$) was significantly higher than the spontaneous ($\bar{\rho} = 0.6635$) and ramp breathing ($\bar{\rho} = 0.7814$). For the inter-subject analysis there were similar trends, where for the coupling Fig. 5 (e) the spontaneous ($\bar{\varepsilon} = 0.7661$) was significantly smaller than all the three control breathing patterns ($\bar{\varepsilon} = 0.8992; 0.9046; 0.8713$), while for the similarity Fig. 5 (f) the sine ($\bar{\rho} = 0.7845$) was significantly greater than spontaneous ($\bar{\rho} = 0.6553$) and ramp ($\bar{\rho} = 0.6883$), and the aperiodic ($\bar{\rho} = 0.7477$) was greater only compared to spontaneous breathing. Similarly to the intra-subject, also for the inter-subject analysis the highest similarity was for the sine breathing.

Furthermore, we wanted to test if there are additional effects, apart from the one induced by the controlled breathing. Therefore, we calculated the residual measures, where we subtracted the mean trend of the specific breathing pattern. For example, for the coupling strength under sine breathing as shown in Fig. 3 (c), we subtracted the mean thick line from all the individual couplings thin grey lines. The boxplots in Fig. 5 (c), (d), (g) and (h) show such residual coupling and similarity for the four breathing patterns. The overall trend for the residual measures is that the higher values for the control breathing are reduced to insignificant difference from the spontaneous breathing. The general conclusion from the residual analysis is that there were no additional (secondary) effects apart from the one that we explicitly induced with the controlled breathing.

4. Discussion

In this work we studied the cardiorespiratory interactions and how they change under controlled time-varying perturbations. We analysed different types of variabilities using methods able to trace the specific variability under observation. We found number of significant differences, some existing trends, and cases where the underlaying interaction mechanisms remain qualitatively unchanged.

The whole investigation was in terms of altering the process of breathing. The motivation comes from the real conditions where various breathing patterns exist, which appear in healthy and disease states [32, 33, 34, 35]. These changes in the breathing patters alter different characteristic, of which, the breathing rate or the frequency often plays one of the key roles. Therefore, we chose to change the breathing frequency in a controlled experimental setting. An important advantage in conducting this protocol was that the subjects are able to easily control the respiration rate through the autonomic nervous system. We used well known time-varying patterns - the ramp, sine and aperiodic variability of the breathing frequency [36, 21]. The goal was to perturb the breathing in a specific and controlled manner and to analyse the resulting interactions in respect and comparison of these pattern variabilities.

With the experimental protocol we introduced explicitly time-variability. The questions we pose and the investigation we conducted about the variabilities were going in the reverse direction – we were averaging different aspect, hence taking out parts of the variabilities and observing how these relate to the introduced perturbation. In particular the variability analysis framework involved: (i) intra-subject variability evaluated by time-averaging, (ii) inter-subject variability evaluated by subject-averaging, and (iii) residual variability evaluated by taking out the trend for the introduced perturbation (in this case time-varying trend). We were able to estimate these variabilities by design of the protocol – the time-varying breathing patterns were tightly controlled and the length of the measurements was the same for all subjects.

In order to analyze the introduced breathing patterns, we needed to use methods that can detect and follow the time-varying dynamics. For this reason we used the wavelet transform for time-frequency analysis [15, 16, 17] and the dynamical Bayesian inference [18, 5] that can model the time-evolving phase dynamics. Moreover, we used a recent version of the later method, called adaptive dynamical Bayesian inference [21], which is particularly optimized for analysis of time-varying dynamics. By modelling the interacting phase dynamics we inferred an effective

connectivity, however, the same framework for variability analysis could be applied also to methods for functional connectivity [37, 38], which could include methods like wavelet coherence or wavelet phase coherence.

It is well known from physiology that variability plays an important role in maintaining healthy functioning in the human body [39, 40, 10, 41]. Important example of such is the cardiovascular variability, which has different mechanisms and aspects, including the RSA, the blood pressure fluctuations and baroreceptor sensitivity, contributing to its complexity [9, 42, 43]. In our study we induced variability in the cardiovascular system by voluntary altering the timing of the breathing in specific ways, in order to model and detect physiological changes. Given the cardiorespiratory input data, we were able to follow directly only the respiratory-related part of the cardiovascular variability [6]. The results indicated several interesting findings about the cardiorespiratory interactions. First, the time-variability from the wavelet analysis of the perturbed respiration signals in Fig. 2 were also present and visually noticeable in the coupling strength analysis in Fig. 3. Due to the introduced breathing temporal variabilities, the coupling functions were varying in time. This was most noticeable for the sine example in Fig. 3. The specific time-variabilities showed that the coupling was large for slow, and small for rapid breathing rates, which goes in line with what was usually observed with RSA in physiological studies [34, 36].

The time-domain coupling analysis showed quite well agreement with the introduced respiratory time-variability, however, when we average across time and different subjects, the resultant coupling functions were qualitatively very similar between the four breathing regimes, as shown in Fig. 4. This demonstrated that the interaction mechanisms defined by the coupling functions remain invariant on average i.e. that when the explicitly introduced breathing variabilities were removed, the mechanism of the interaction remains the same regardless of the breathing pattern. The specific form of this coupling function is of direct form depending predominantly on the respiration phase [5, 8, 44]. One should note here, that this models the deterministic part related to the input of the respiration data and can be used for characterization of the RSA, whereas the other residual noisy part is independent of respiration and beside the random perturbations reflects also possible intrinsic sources of HRV as well as the effects of other unobserved rhythms like baroreflex or angiotensin loop rhythms [6].

The quantitative time-averaged statistical comparisons in Fig. 5 showed similar results. Namely, there were significantly increased couplings and similarities for both the intra-subject and inter-subject analysis, where different breathing regimes were more or less predominant. However, when we estimated the residual couplings and similarities by removing the introduced time-variability, then nothing was significantly higher than the spontaneous free breathing. Integrating the main results of Fig. 4 and Fig. 5 that on time-average: (i) the coupling functions are the same for different breathing and (ii) the residual coupling and similarity are not different than the spontaneous breathing, implies that the main interaction mechanism is qualitatively and quantitatively invariant on average outside the scope of what was introduced by the time-varying breathing perturbations protocols. Thus, even though the coupling function is varying in time due to breathing perturbations (as in Fig. 3), when time-averaged it has fairly stable and invariant form (as shown in Fig. 4 and Fig. 5). We note, however, that these results are for healthy control subjects, and there could be some deviations from the main coupling form if time-average coupling function are investigated for patients with some different breathing patterns or cardiovascular disease.

In this work we discuss the variability framework in light of the two oscillations in the cardiorespiratory interaction. Needless to say, however, the whole variability framework is readily applicable more generally to other interacting (oscillatory) systems and networks.

CRediT authorship contribution statement

D. Lukarski: Methodology, Formal analysis, Writing - Original Draft, Writing - Review & Edit-

ing. **D. Stavrov:** Data Curation, Formal analysis, Visualization. **T. Stankovski:** Conceptualization, Methodology, Writing - Original Draft, Writing - Review & Editing, Supervision.

Acknowledgments

We acknowledge valuable support and access to facilities from the Institute of Pathophysiology Nuclear Medicine, at Faculty of Medicine Skopje, Macedonia.

Declaration of Competing Interest

The authors declare that they have no known competing financial interests or personal relationships that could have appeared to influence the work reported in this paper.

References

[1] L. H. Opie, Heart physiology: from cell to circulation, Lippincott Williams & Wilkins, 2004.

[2] R. M. Berne, Cardiovascular physiology, Annual Review of Physiology 43 (1) (1981) 357–358.

[3] C. Schäfer, M. G. Rosenblum, J. Kurths, H. H. Abel, Heartbeat synchronised with ventilation, Nature 392 (6673) (1998) 239–240.

[4] A. Stefanovska, H. Haken, P. V. E. McClintock, M. Hožič, F. Bajrović, S. Ribarič, Reversible transitions between synchronization states of the cardiorespiratory system, Phys. Rev. Lett. 85 (22) (2000) 4831–4834.

[5] T. Stankovski, A. Duggento, P. V. E. McClintock, A. Stefanovska, Inference of time-evolving coupled dynamical systems in the presence of noise, Phys. Rev. Lett. 109 (2012) 024101.

[6] B. Kralemann, M. Frühwirth, A. Pikovsky, M. Rosenblum, T. Kenner, J. Schaefer, M. Moser, In vivo cardiac phase response curve elucidates human respiratory heart rate variability, Nat. Commun. 4 (2013) 2418.

[7] S. Schulz, J. Haueisen, K.-J. Bär, A. Voss, Multivariate assessment of the central-cardiorespiratory network structure in neuropathological disease, Physiological measurement 39 (7) (2018) 074004.

[8] D. Iatsenko, A. Bernjak, T. Stankovski, Y. Shiogai, P. J. Owen-Lynch, P. B. M. Clarkson, P. V. E. McClintock, A. Stefanovska, Evolution of cardio-respiratory interactions with age, Phil. Trans. R. Soc. Lond. A 371 (1997) (2013) 20110622.

[9] J. A. Hirsch, B. Bishop, Respiratory sinus arrhythmia in humans – How breathing pattern modulates heart rate, Am. J. Physiol. 241 (4) (1981) H620–H629.

[10] G. G. Berntson, J. T. Bigger, D. L. Eckberg, P. Grossman, P. G. Kaufmann, M. Malik, H. N. Nagaraja, S. W. Porges, P. H. Saul, J. P. Stone, M. W. VanderMolen, Committee report: heart rate variability: origins, methods, and interpretive caveats, Psychophysiology 34 (1997) 623–648.

[11] A. Voss, S. Schulz, R. Schroeder, M. Baumert, P. Caminal, Methods derived from nonlinear dynamics for analysing heart rate variability, Philosophical Transactions of the Royal Society A: Mathematical, Physical and Engineering Sciences 367 (1887) (2009) 277–296.

[12] M. B. Lotrič, A. Stefanovska, D. Štajer, V. Urbančič-Rovan, Spectral components of heart rate variability determined by wavelet analysis, Physiol. Meas. 21 (2000) 441–457.

[13] R. Pernice, M. Javorka, J. Krohova, B. Czippelova, Z. Turianikova, A. Busacca, L. Faes, et al., Comparison of short-term heart rate variability indexes evaluated through electrocardiographic and continuous blood pressure monitoring, Medical & biological engineering & computing 57 (6) (2019) 1247–1263.

[14] S. Ghiasi, A. Greco, R. Barbieri, E. P. Scilingo, G. Valenza, Assessing autonomic function from

electrodermal activity and heart rate variability during cold-pressor test and emotional challenge, Scientific Reports 10 (1) (2020) 1–13.

[15] I. Daubechies, Ten lectures on wavelets, SIAM, 1992.

[16] G. Kaiser, A Friendly Guide to Wavelets, Birkhäuser, Boston, 1994.

[17] A. Stefanovska, M. Bračič, H. D. Kvernmo, Wavelet analysis of oscillations in the peripheral blood circulation measured by laser Doppler technique, IEEE Trans. Bio. Med. Eng. 46 (10) (1999) 1230–1239.

[18] V. N. Smelyanskiy, D. G. Luchinsky, A. Stefanovska, P. V. E. McClintock, Inference of a nonlinear stochastic model of the cardiorespiratory interaction, Phys. Rev. Lett. 94 (9) (2005) 098101.

[19] T. Stankovski, T. Pereira, P. V. E. McClintock, A. Stefanovska, Coupling functions: Universal insights into dynamical interaction mechanisms, Rev. Mod. Phys. 89 (33) (2017) 045001.

[20] T. Stankovski, T. Pereira, P. V. McClintock, A. Stefanovska, Coupling functions: dynamical interaction mechanisms in the physical, biological and social sciences, Philosophical transactions. Series A, Mathematical, physical, and engineering sciences 377 (2160).

[21] D. Lukarski, M. Ginovska, H. Spasevska, T. Stankovski, Time window determination for inference of time-varying dynamics: application to cardiorespiratory interaction, Frontiers in Physiology 11.

[22] D. Iatsenko, P. V. E. McClintock, A. Stefanovska, On the extraction of instantaneous frequencies from ridges in time-frequency representations of signals, Signal Proc. 125 (2016) 290–303.

[23] E. N. Lorenz, Deterministic non-periodic flow, J. Atmos. Sci. 20 (2) (1963) 130–141.

[24] Y. Kuramoto, Chemical Oscillations, Waves, and Turbulence, Springer-Verlag, Berlin, 1984.

[25] H. Nakao, T. Yanagita, Y. Kawamura, Phase-reduction approach to synchronization of spatiotemporal rhythms in reaction-diffusion systems, Phys. Rev. X 4 (2) (2014) 021032.

[26] A. Duggento, T. Stankovski, P. V. E. McClintock, A. Stefanovska, Dynamical Bayesian inference of time-evolving interactions: From a pair of coupled oscillators to networks of oscillators, Phys. Rev. E 86 (2012) 061126.

[27] T. Stankovski, A. Duggento, P. V. E. McClintock, A. Stefanovska, A tutorial on time-evolving dynamical Bayesian inference, Eur. Phys. J. Special Topics 223 (13) (2014) 2685–2703.

[28] B. Kralemann, L. Cimponeriu, M. Rosenblum, A. Pikovsky, R. Mrowka, Phase dynamics of coupled oscillators reconstructed from data, Phys. Rev. E 77 (6, Part 2) (2008) 066205.

[29] T. Schreiber, H. Kantz, Predictability of complex dynamical systems, in: Observing and Predicting Chaotic Signals, Springer, New York, 2003.

[30] G. Lancaster, D. Iatsenko, A. Pidde, V. Ticcinelli, A. Stefanovska, Surrogate data for hypothesis testing of physical systems, Phys. Rep.

[31] T. Stankovski, V. Ticcinelli, P. V. E. McClintock, A. Stefanovska, Neural cross-frequency coupling functions, Front. Syst. Neurosci. 11 (33) (2017) 10.3389/fnsys.2017.00033.

[32] M. J. Tobin, T. S. Chadha, G. Jenouri, S. J. Birch, H. B. Gazeroglu, M. A. Sackner, Breathing patterns: 1. normal subjects, Chest 84 (2) (1983) 202–205.

[33] M. J. Tobin, T. S. Chadha, G. Jenouri, S. J. Birch, H. B. Gazeroglu, M. A. Sackner, Breathing patterns: 2. diseased subjects, Chest 84 (3) (1983) 286–294.

[34] D. L. Eckberg, The human respiratory gate, J. Physiol. (London) 548 (2) (2003) 339–352.

[35] M. Ragnarsdóttir, E. K. Kristinsdóttir, Breathing movements and breathing patterns among healthy men and women 20–69 years of age, Respiration 73 (1) (2006) 48–54.

[36] T. Stankovski, W. H. Cooke, L. Rudas, A. Stefanovska, D. L. Eckberg, Time-frequency methods and voluntary ramped-frequency breathing: a powerful combination for exploration of human neurophysiological mechanisms, J. Appl. Physiol. 115 (12) (2013) 1806–1821.

[37] K. J. Friston, Functional and effective connectivity: a review, Brain. Connect. 1 (1) (2011) 13–36.

[38] H.-J. Park, K. Friston, Structural and functional brain networks: from connections to cognition, Science 342 (6158) (2013) 1238411.

[39] R. B. Stein, E. R. Gossen, K. E. Jones, Neuronal variability: noise or part of the signal?, Nature Reviews Neuroscience 6 (5) (2005) 389–397.

[40] J. M. Karemaker, K. H. Wesseling, Variability in cardiovascular control: the baroreflex reconsidered, Cardiovascular engineering 8 (1) (2008) 23–29.

[41] S. C. Malpas, Neural influences on cardiovascular variability: possibilities and pitfalls, Am. J. Physiol.: Heart. Circ. Physiol. 282 (2002) H6–H20.

[42] D. L. Eckberg, Point: Counterpoint: Respiratory sinus arrhythmia is due to a central mechanism vs. respiratory sinus arrhythmia is due to the baroreflex mechanism, J. Appl. Physiol. 106 (5) (2009) 1740–1742.

[43] J. M. Karemaker, Last word on point: counterpoint: respiratory sinus arrhythmia is due to a central mechanism vs. respiratory sinus arrhythmia is due to the baroreflex mechanism, Journal of applied physiology (2009) 1750.

[44] T. Stankovski, S. Petkoski, J. Raeder, A. F. Smith, P. V. E. McClintock, A. Stefanovska, Alterations in the coupling functions between cortical and cardio-respiratory oscillations due to anaesthesia with propofol and sevoflurane., Phil. Trans. R. Soc. A 374 (2067) (2016) 20150186.